MODIFICATION OF THE WYLLIE TIME SERIES ACOUSTIC EQUATION, TO GIVE A RIGOROUS SOLUTION IN THE PRESENCE OF GAS

M. Holmes, A. Holmes and D. Holmes, Digital Formation, Inc., Denver, Colorado

This paper was prepared for presentation at the SPWLA 45th Annual Logging Symposium held in Noordwijk, The Netherlands, June 6–9, 2004.

ABSTRACT

Gassmann's equation has been used in seismic analysis for a number of decades to quantify the effect of gas on the slowing of rock velocity. It is well known that low gas saturations have a large effect on velocity slowing, in a pronounced non-linear fashion. In petrophysical analyses, Wyllie's Time Series Equation cannot account for the Gassmann behavior by simply adjusting the fluid travel time of the gas/liquid mixture.

Gassmann's approach is here extended into the shaley formation realm, and the effect of velocity slowing is merged with the Wyllie Time Series Equation. This is accomplished by treating the liquid filled porosity separately from the gas filled porosity. Terms needed to solve Gassmann's equation are the volumes of porosity, fluids, matrix and clay, along with their elastic moduli. All parameters are available from look up tables and/or calculations knowing fluid composition and reservoir pressure.

The methodology consists of calculating a shaley formation model of porosity (best is from combined density/neutron log readings), fluid saturation and clay volume. Models for both wet rocks and the uninvaded gas-bearing zone are constructed, yielding pseudo acoustic compressional curves for each case.

Knowing the mixture of gas and water in the uninvaded zone, it is then possible to determine a "pseudo travel time" for the fluid mixture to satisfy the traditional Wyllie Time Series Equation. For all reservoir systems examined, and for the entire range of porosity and for shale volumes up to about 70%, there are excellent hyperbolic relations between the bulk volume of gas and the "pseudo travel time." The shape and position of the hyperbola can be defined by three constants that vary from one reservoir to the next. By incorporating these constants appropriately into the Wyllie Time Series Equation, a gas term is established, which rigorously reproduces the Gassmann effect. At zero gas saturation the gas term becomes zero, and Wyllie's Time Series Equation reverts to its original form.

An important observation is that, in gas/liquid systems, the acoustic log cannot be used reliably to calculate porosity, unless there is independent knowledge of gas saturation.

Examples are presented from five reservoirs, four clastic and one carbonate.

INTRODUCTION

Most of the research into the effects of gas on acoustic properties of rock systems has been oriented towards understanding seismic responses. Domenico (1974, 1976) investigated changes in acoustic velocity as a function of gas saturation, and Gassmann (1951) developed a model relating elastic and bulk moduli of rock and fluids to acoustic velocity. These analyses demonstrated that even very low saturations of gas affect acoustic velocities (slowing of velocity or increasing acoustic travel time) in a remarkably non-linear fashion.

The original Wyllie Time Series Equation (Wyllie et al, 1956) assumes a binary rock model consisting of matrix and porosity:

$$DT = \underbrace{(1-\phi)\times DT_{ma}}_{Matrix} + \underbrace{\phi \times DT_f}_{Fluid}$$

Where:

DT	Acoustic Travel Time
ϕ	Porosity
DT_{ma}	Travel time of the rock matrix
DT_f	Travel time of the fluid within the pore space

If the rock is saturated with water or oil, acoustic travel time is relatively constant (189 microseconds per foot, or 620 microseconds per meter). However, if gas is present in the pore space within the zone measured by the acoustic device, then DT_f will increase. Moreover, the increase is not a simple proportionality to the relative volumes of gas and liquid.

These findings demonstrate that there is no rigorous way to incorporate gas saturation into standard petrophysical treatment of acoustic log analysis. Schlumberger (1989) suggests empirical adjustments to standard analyses – for example, multiply porosity by 0.7 to account for increases in acoustic travel time in the presence of gas.

GASSMANN ANALYSIS

Gassmann's Equation can be expressed in a way suitable for petrophysical analysis (Crain 1986):

$$M = M_{erf} + \frac{\left[1 - \frac{B_{erf}}{B_{Solid}}\right]}{\frac{\phi_T}{B_f} + \frac{1-\phi_T}{B_{Solid}} + \frac{B_{erf}}{B_{Solid}^{\ 2}}}$$

$$V_P = \left(\frac{M}{\rho_B}\right)^{0.5}$$

Where:

M	Elastic Modulus of the porous fluid filled rock
M_{erf}	Elastic Modulus of the empty rock frame
B_{erf}	Bulk Modulus of the empty rock frame
B_{Solid}	Bulk Modulus of the rock matrix and shale
B_f	Bulk Modulus of the fluid in pores and in clay porosity
ϕ_T	Total Porosity
ρ_B	Bulk Density of the rock, fluid, shale combination
V_P	Compressional wave velocity

Solids elastic moduli and bulk moduli can be determined knowing rock matrix and shale properties. Fluid bulk modulus is determined for any assumed saturating fluid combination – oil, gas, water – and using reservoir pressure as input.

Initial processing consists of standard calculations of:

- Porosity – derived from density/neutron combination to minimize changing matrix properties and fluid content
- Matrix Volume
- Shale Volume
- Fluid saturation – oil, gas, water

Theoretical acoustic compressional travel time can then be determined for any desired fluid combination by solving Gassmann's equation. This permits analysis of sensitivity of fluid combination on acoustic responses. Theoretical wet formation response — hereafter called DT_{GW} — can be compared with responses in rock with varying gas saturations.

QUANTIFYING EFFECTS OF GAS

For gas-bearing formations calculations can be made of Gassmann compressional travel times in the uninvaded zones – hereafter called DT_{GU}. Combining this with DT_{ma} and ϕ, the effective fluid travel time, $DT_{f\ eff}$, can be determined from the Wyllie Time Series Equation:

$$DT_{GU} = (1-\phi) \times DT_{ma} + \phi \times DT_{f\,eff}$$

Knowing gas saturation, Sg, and $DT_{f\ eff}$, solve for effective travel time of gas, here termed DT_{GG}:

$$DT_{GG} = DT_{f\,eff} - Sg \times DT_{GU} + (1 - Sg) \times DT_W$$

Where:

DT_W	Travel time of water

Plots of **Gas Saturation (Sg) vs. DT_{GG}** (**Figures 1**, **3**, **5**, **7**, **9**) and **Bulk Volume Gas ($\phi \times Sg$) vs. DT_{GG}** show strong hyperbolic relationships. Also, plots of the gas saturation versus the ratio of DT_{GU} to DT_{GW} demonstrate clearly the non-linear velocity slowing as a consequence of gas saturation (**Figures 2**, **4**, **6**, **8**, **10**).

ADDING A GAS TERM TO THE WYLLIE TIME SERIES EQUATION

The relation between bulk volume of gas $(\phi \times Sg)$ and effective travel time of gas, DT_{GG} can be expressed by the general equation:

$$(\phi \times Sg - C1) \times (DT_{GG} - C2) = C3$$

Where C1, C2 and C3 are constants, and vary from one reservoir to the next. C1 and C2 do not generally show much change, but C3 is strongly porosity dependent (**Figure 11**).

This correlation allows for the addition of a gas term to the Wyllie Time Series Equation (clean formation):

$$DT = \left[\frac{\phi \times Sg \times C3}{\phi \times Sg - C1} + C2 \times \phi \times Sg\right]$$
Gas Term
$$+ \left[(1-\phi) \times DT_{ma}\right]$$
Matrix Term
$$+ \left[\phi \times S_W \times DT_W\right]$$
Water Term

For many reservoirs, C1 is very small, and can be ignored, in which case the equation reduces to:

$$DT = \left[C3 + C2 \times \phi \times Sg\right]$$
Gas Term
$$+ \left[(1-\phi) \times DT_{ma}\right]$$
Matrix Term
$$+ \left[\phi \times S_W \times DT_W\right]$$
Water Term

Shale effects can be incorporated:

$$DT = \left[\frac{\phi_e \times Sg \times C3}{\phi_e \times Sg - C1} + C2 \times \phi_e \times Sg\right]$$
Gas Term
$$+ \left[(1-V_{SH}) \times (1-\phi_e) \times DT_{ma}\right]$$
Matrix Term
$$+ \left[\phi_e \times S_W \times DT_W\right]$$
Water Term
$$+ \left[V_{SH} \times DT_{SH}\right]$$
Shale Term

Where:

ϕ	Porosity, undifferentiated
ϕ_e	Effective Porosity, here termed as total porosity less clay porosity
S_W	Water Saturation
V_{SH}	Volume of Shale
DT_{ma}	Travel Time of Matrix
DT_{SH}	Travel Time of Shale
Sg	Gas Saturation

When no gas is present, the gas term is zero, and the equation reverts to the original Wyllie Time Series Equation.

Application of this equation will converge on the DT_{GU} or DT_{GW} curves.

RESULTS: SOLVING FOR THE GAS TERM

Results from 5 different reservoirs are presented:

Shell OCSG7954 #1
Offshore Gulf Coast USA, high porosity sands

CSM Strat Test #61
Wyoming, high porosity sands

Cameron Parish Louisiana
Louisiana, medium porosity sands

LA-Lime
Louisiana, medium porosity limestone

Wamsutter
Wyoming, low porosity sands

Figures 1, **3**, **5**, **7** & **9** show the best-fit shifted hyperbolic functions of **Bulk Volume Gas ($\phi \times Sg$) vs. DT Gassmann - Gas (DT_{GG})**. A summary of the parameters for the shifted hyperbolae is presented in **Table 1**.

A plot of **Average Porosity vs. C3** is shown in **Figure 11**; in general, there is a pronounced increase in C3 as average porosity increases.

RESULTS: GASSMANN THEORETICAL CURVES

Bulk Volume Gas ($\phi \times Sg$) vs. DT Gassmann - Gas (DT_{GG})
Figures 1, **3**, **5**, **7**, & **9** used to calculate the hyperbolic functions show this data. All wells show excellent correlation. Two of the wells (CSM Strat Test #6, and Wamsutter) show some data

dispersion that is at least partly controlled by the absolute value of porosity. However the ordering is different for each well – CSM Strat Test #61 has lowest value for C3 for the high porosities, whereas Wamsutter shows the reverse.

Gas Saturation (Sg) vs. Ratio DT_{GU} to DT_{GW}

All wells show a similar pattern (**Figures 2**, **4**, **6**, **8** & **10**) – a rapid increase in the ratio at low gas saturation, with a relatively constant ratio throughout the remaining levels of gas saturation. At very high gas saturations, it decreases slightly. However, details of the correlation change, and one well – CSM Strat Test #61 – shows a great deal of data dispersion (for no obvious reason). A summary is in **Table 2**.

In general, it appears that the ratios increase with increasing average porosity.

RESULTS: COMPARISONS OF GASSMANN, WYLLIE THEORETICAL CURVES WITH MEASURED DT COMPRESSIONAL DATA

Figures 13-17 are depth plots for all wells showing the following data:

- Shale, matrix, oil, gas, water
- Raw resistivity logs
- Raw porosity logs
- Comparison among measured DT, DT_{GW} and DT_{GU}. Difference between the two Gassmann curves highlighted
- Comparison between DT_{GW} and DT_{WW}, with differences highlighted.

Shell OCSG7954 #1 (Figure 13)

The thick sand, from 15440 feet to 15615 feet has porosities ranging from 25% to 35%, and gas saturation from 25% to 75%. Density/neutron response indicates gas effects. Difference between DT_{GU} and DT_{GW} is about 40 microseconds per foot. Measured acoustic compressional DT is mostly between these two theoretical curves, suggesting that the acoustic log is variably affected by gas, i.e. residual gas saturation as "seen" by the acoustic log is quite variable.

There is good correspondence between DT_{GU} and DT_{WU} for this and all other wells.

CSM Strat Test #61 (Figure 14)

Sands between 100 feet and 230 feet have porosities ranging from 10% to 33%, and gas saturation from 40% to 90%. These shallow sands are actually filled with air (above the water table). Difference between DT_{GW} and DT_{GU} is about 50 microseconds per foot, and the measured acoustic compressional curve is mostly quite close to DT_{GU}. This suggests little to no invasion by mud filtrate (acoustic logs "sees" the uninvaded zone).

Cameron Parish Louisiana (Figure 15)

Sands between 13885 feet and 13990 feet have porosities ranging from 5% to 20% - significantly lower than the previous two examples. Gas saturation is from 25% to 80%. There is only relatively minor separation (10 microseconds per foot) between DT_{GU} and DT_{GW}. Measured acoustic compressional DT meanders between the two theoretical curves, suggesting a quite variable mud filtrate invasion profile as it affects the measured acoustic log.

LA-Lime (Figure 16)

A limestone reef occurs between 7990 feet and 8155 feet. The hydrocarbon accumulation consists of a gas cap (to 8065 feet) overlying an oil leg (to 8095 feet) with water and small amounts of residual oil below. Porosity in the limestone which is hydrocarbon bearing is from 15% to 22%. Within the gas cap, gas saturation is from 20% to 40%.

Difference between DT_{GU} and DT_{GW} is about 10 microseconds per foot. Measured acoustic compressional DT meanders between the two theoretical curves. In the oil leg and below the oil/water contact, it coincides with DT_{GW} (as it should).

Wamsutter (Figure 17)

A series of sands below 9835 feet have porosities ranging from 3% to 10%, and gas saturation from 0% to 40%. Separation between DT_{GU} and DT_{GW} is less than 10 microseconds per foot. Measured acoustic compressional DT meanders between the two theoretical curves, suggesting a varied mud filtrate invasion as "seen" by the acoustic log.

MATRIX PROPERTIES

Matrix Properties used for the Gassmann theoretical DT Compressional curves (DT_{GG}) are presented in **Table 3**.

DT_{ma} values were chosen such that the theoretical Gassmann curves show logical correlation with measured DT compressional curves.

The values of DT_{ma} for the two high porosity sand examples are outside the range of values normally used. **Figure 12** shows the DT_{ma} transforms used for the two high porosity sands, compared with Bcp – compaction curves for unconsolidated sands – suggesting both examples to have Bcp values ranging from about 1.3 to 1.6. However, the approach used here does not require independent calculations of Bcp. Additionally, for these two examples, DT_{ma} values are "pseudo", and are a result of under-compaction.

CONCLUSIONS

1. A petrophysical solution to the Gassmann acoustic fluid substitution model is presented, which allows deterministic modeling of theoretical compressional acoustic curves for any desired fluid combination of gas and water.
2. Knowing the mixture of gas and water, it is possible to determine effective travel times of the gas/water fluid system. This, in turn, allows for modification of the Wyllie Time Series Equation to include a gas term.
3. Analysis of five reservoirs (four sand reservoirs with different porosity ranges, and one limestone) shows that the increase of compressional travel time due to the presence of gas is strongly porosity dependent. For high porosity reservoirs (25% to 35% porosity), DT compressional increases by some 40 to 50 microseconds per foot. The increase is a non-linear function of gas saturation. For low porosity reservoirs (20% and less) increase of DT compressional is 10 microseconds per foot or less.
4. Comparison of measured DT compressional with the theoretical Gassmann curves suggest that invasion by mud filtrate is quite variable, and the amount of gas as "seen" by the acoustic log has a wide range. The important corollary is that it cannot be assumed that acoustic logs always respond to residual gas. This has significant implication in using acoustic logs for the generation of synthetic seismograms in gas-bearing sequences.
5. Recreated theoretical acoustic curves using the newly-developed Wyllie Time Series Equation (to include a gas term) are very close to the theoretical Gassmann modeled curves.
6. The approach presented incorporates a "pseudo" DT_{ma} to account for under-compacted sands.

REFERENCES

Crain, E.R,: 1986, "The Log Analysis Handbook, Volume 1," p. 583

Domenico, S.N.: "Effect of Brine-Gas Mixture on Velocity in an Unconsolidated Sand Reservoir," Geophysics (October 1976), p. 882

Domenico, S.N.: "Effect of Water Saturation on Seismic Reflectivity of Sand Reservoirs Encased in Shale," Geophysics (December 1974), p. 759

Gassmann, F.: 1951, "Über die Elastizität poröser Medien," Vier. Der Natur. Gesellschaft in Zürich, 96, 1-23

Schlumberger: 1989, "Log Interpretation Principles/Applications, 2nd Version", p. 5-7

Wyllie, M.R.J., Gregory, A.R., Gardner, G.H.F., "Elastic Wave Velocities in Heterogeneous and Porous Media," Geophysics (January 1956), p. 41-70

ABOUT THE AUTHORS

Michael Holmes has a Ph.D. from the University of London in geology and a MSc. from the Colorado School of Mines in Petroleum Engineering. His professional career has involved employment with British Petroleum, Shell Canada, Marathon Oil Company and H.K. van Poollen and Associates. For the past 15 years he has worked on petrophysical analyses for reservoirs worldwide under the auspices of Digital Formation, Inc.

Antony M. Holmes has a BS in Computer Science from the University of Colorado. He has been involved with the development of petrophysical software for 15 years with Digital Formation, Inc., particularly with regards to the implementation of petrophysical analyses.

Dominic I. Holmes has a BS in Chemistry and a BS in Mathematics from the Colorado School of Mines. He has been involved with the development of petrophysical software for 15 years with Digital Formation, Inc., particularly with regards to the presentation of petrophysical information in a graphical format.

Well	C1	C2	C3	Average Porosity %	Correlation Coefficient, R2
Shell OCSG7954 #1	-0.0303	172.4	41.04	31	0.977
CSM Strat Test #61	-0.0015	157.9	59.57	28	0.946
Cameron Parish Louisiana	0.0133	209.7	7.73	17	0.854
LA-Lime	-0.0144	149.3	17.19	21	0.920
Wamsutter	-0.0019	191.2	11.47	7	0.889
Average	**-0.0070**	**176.1**	**27.40**		

Table 1 - Summary of the Hyperbolic Equations of Bulk Volume of Gas ($\phi \times Sg$) vs. DT Gassmann - Gas (DT_{GG}).

Well	Average Porosity %	Ratio at Sg							
		0.1	0.2	0.3	0.4	0.5	0.6	0.7	0.8
Shell OCSG7954 #1	31	1.16	1.24	1.27	1.28	1.29	1.29	1.28	-
CSM Strat Test #61	28	1.15	1.20	1.24	1.26	1.29	1.30	-	-
Cameron Parish Louisiana	17	1.09	1.11	1.12	1.13	1.13	1.13	1.13	1.125
LA-Lime	21	1.11	1.12	1.13	1.14	1.15	1.15	1.13	1.12
Wamsutter	7	1.13	1.16	1.17	1.17	1.17	1.16	1.16	1.15

Table 2 - Summary of the Ratio of DT_{GU} / DT_{GW} values at different values of Sg.

Well	DT_{ma}	$DT_{Clay\ Solids}$
Shell OCSG7954 #1	80	55
CSM Strat Test #61	75	110
Cameron Parish Louisiana	50	40
LA-Lime	45	55
Wamsutter	50	50

Table 3 -Matrix Properties used for the Gassmann theoretical DT Compressional curves (DT_{GG}).

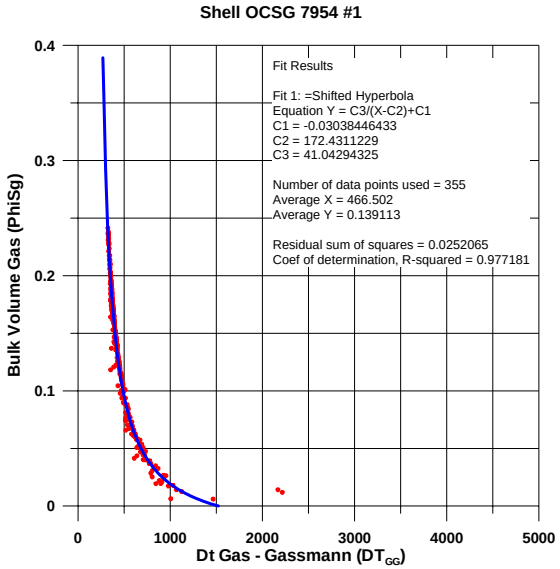

Figure 1 - Shell OCSG7954 #1. Shows excellent correlation.

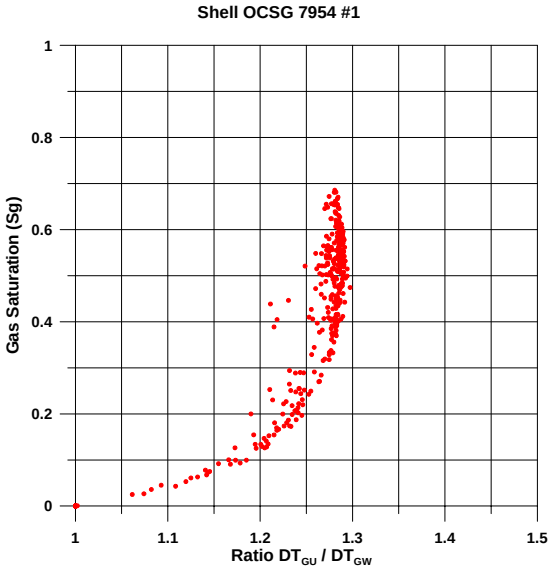

Figure 2 - ShellOCSG 7954 #1. The dispersed data has high V_{SH} (> 30%).

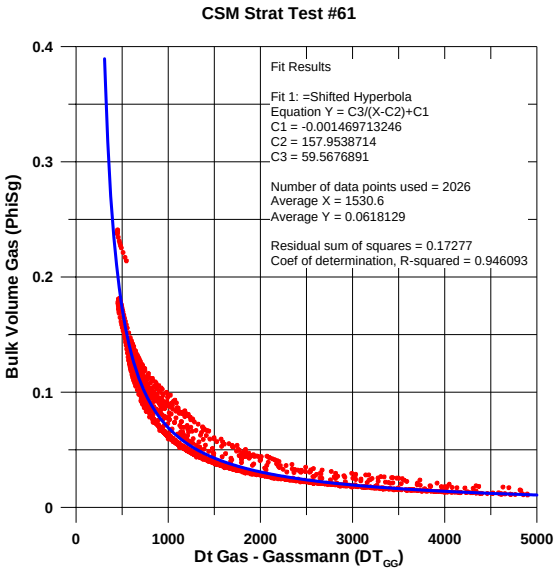

Figure 3 - CSM Strat Test #61. The points above the main data trend are lower porosity.

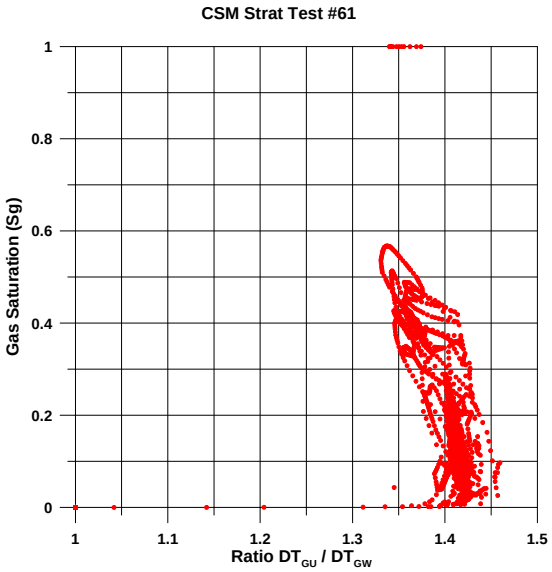

Figure 4 - CSM Strat Test #61. The data dispersion is from lower porosity points.

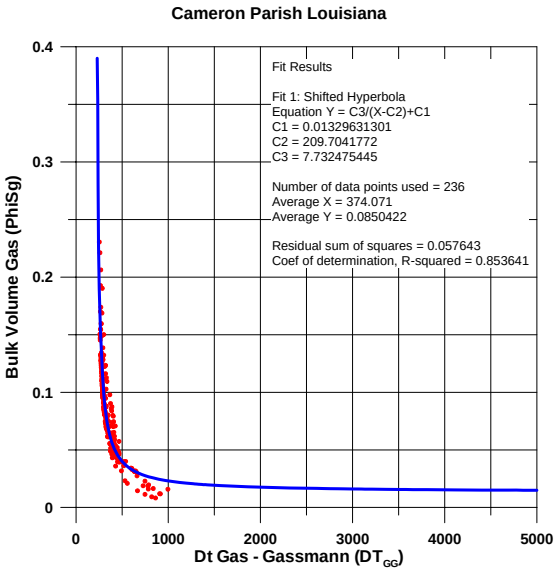

Figure 5 - Cameron Parish Louisiana. Shows excellent correlation.

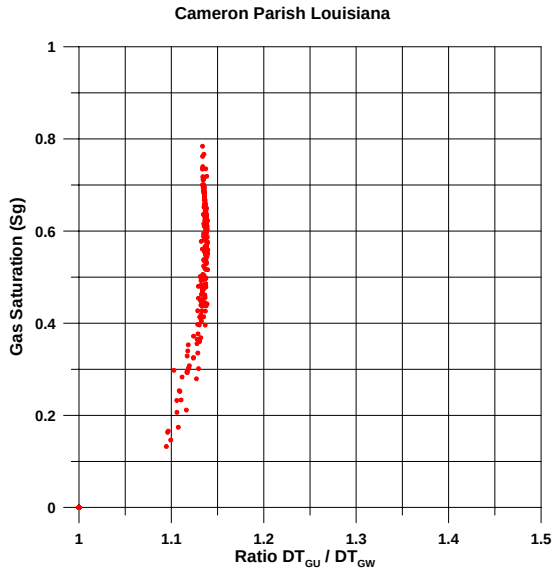

Figure 6 - Cameron Parish Louisiana. Shows excellent correlation.

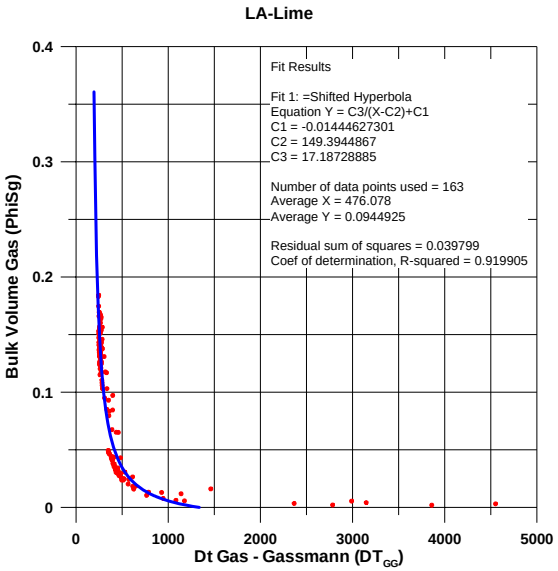

Figure 7 - LA-Lime. Shows excellent correlation.

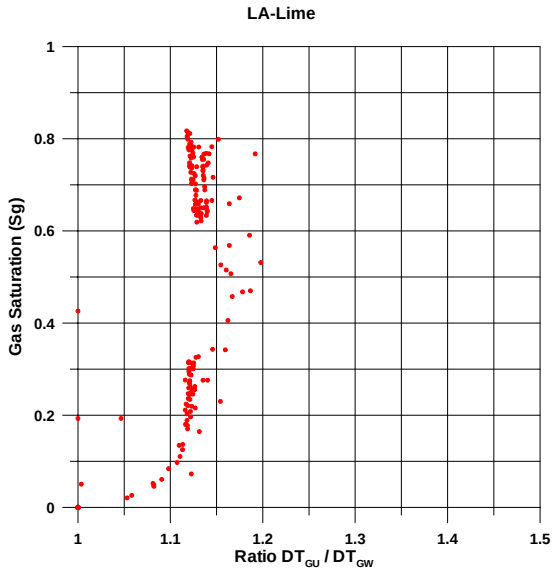

Figure 8 - LA-Lime. Shows good correlation, except in gas saturations from 30% - 60%.

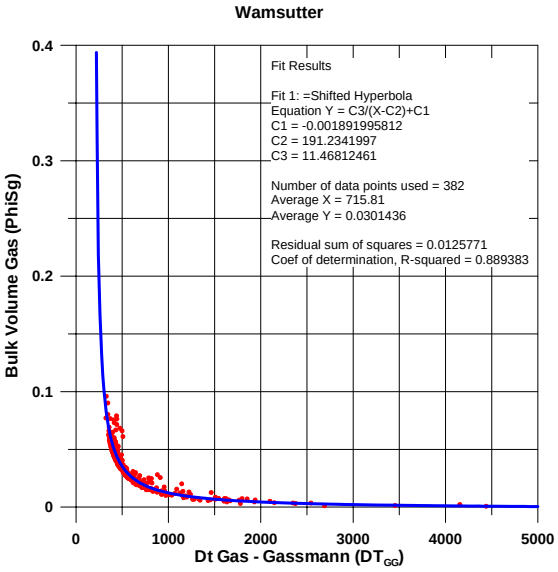

Figure 9 - Wamsutter. Shows excellent correlation.

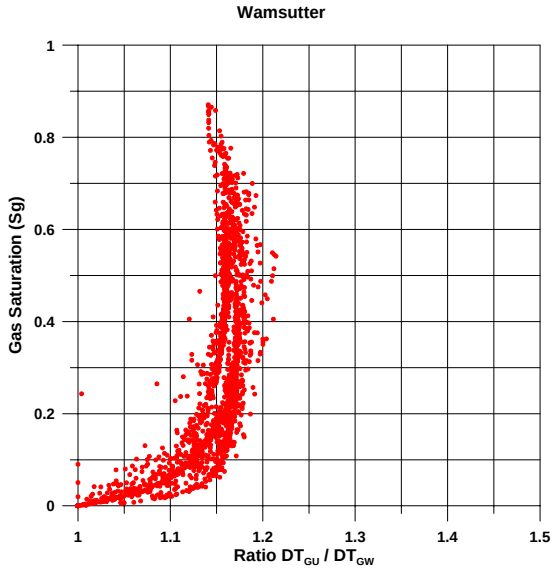

Figure 10 - Wamsutter. The data dispersion is not related to porosity or V_{SH}.

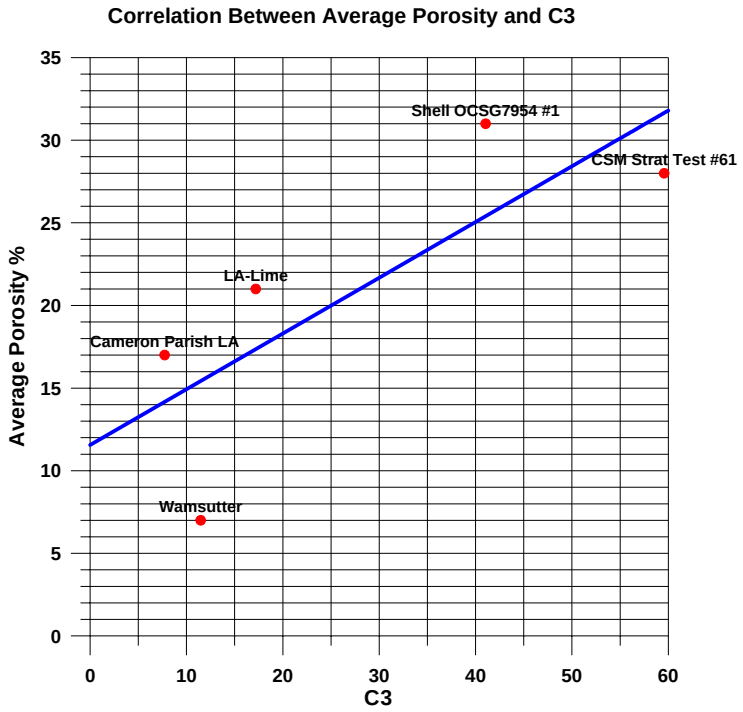

Figure 11 - Average porosities of the 5 examples compared to the C3 parameter.

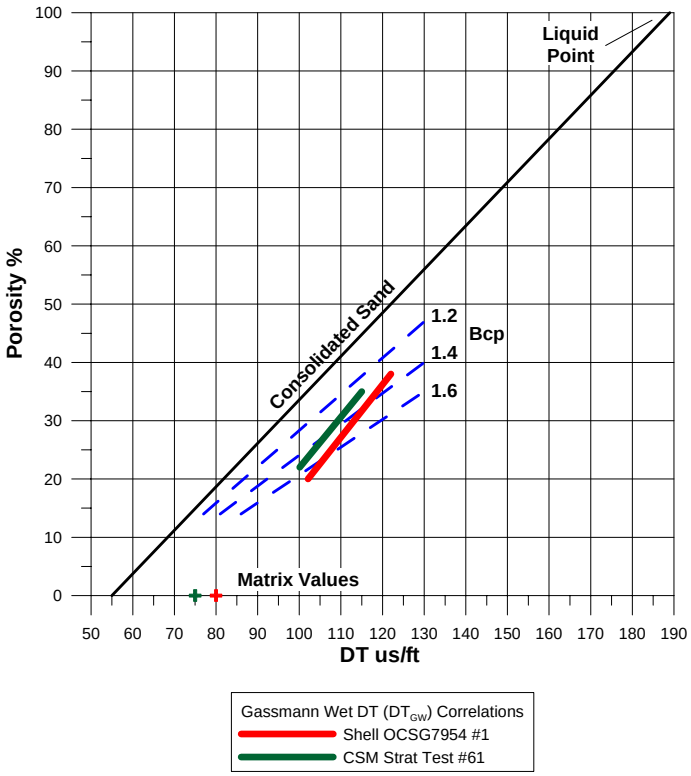

Figure 12 - Comparison of porosity with Gassmann Wet DT (DT_{GW}), and the interpretation of under-compacted sands.

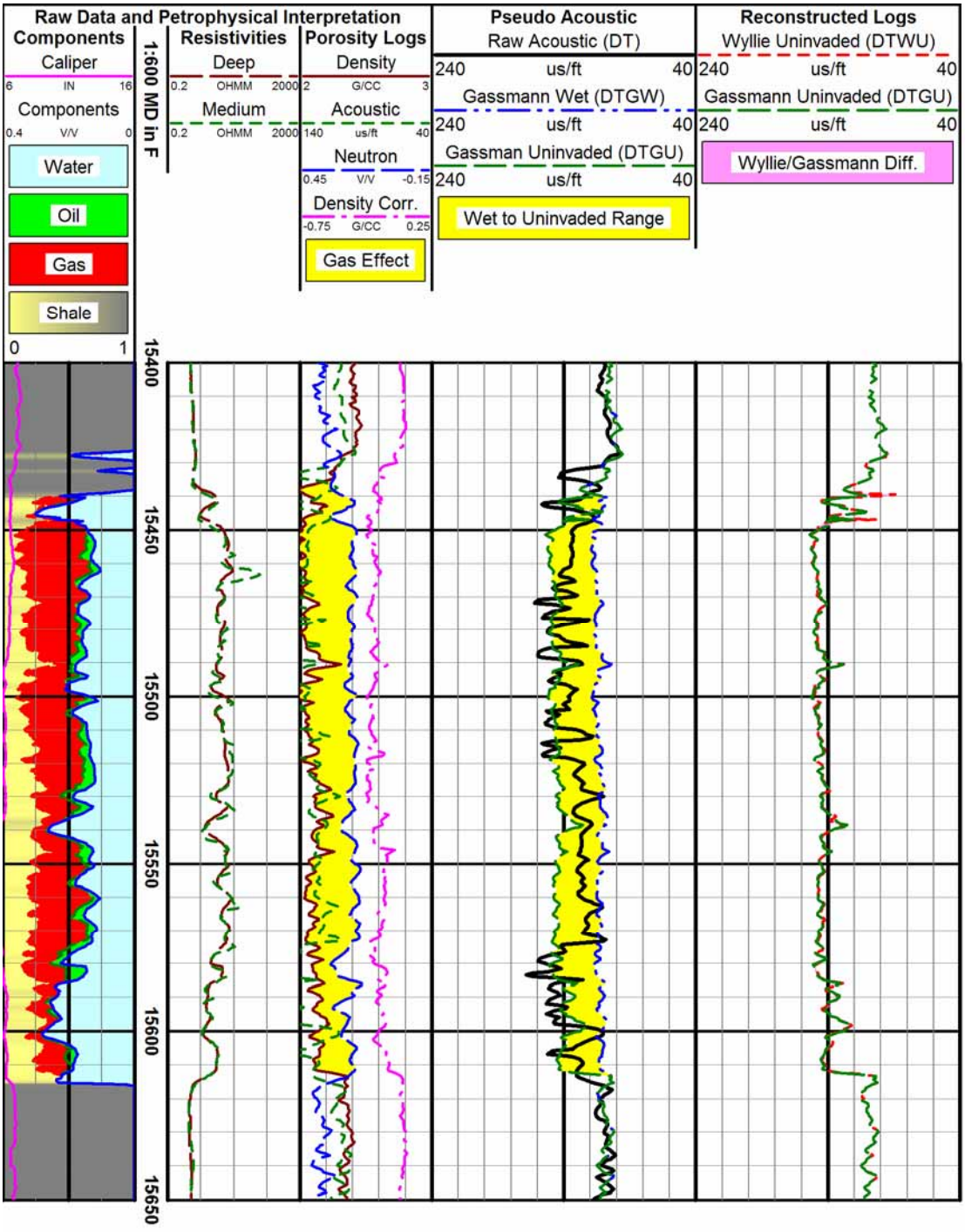

Figure 13 - Shell OCSG7954 #1. The difference between DT_{GU} and DT_{GW} is approximately 40 microseconds per foot. The actual DT meanders between DT_{GU} and DT_{GW}.

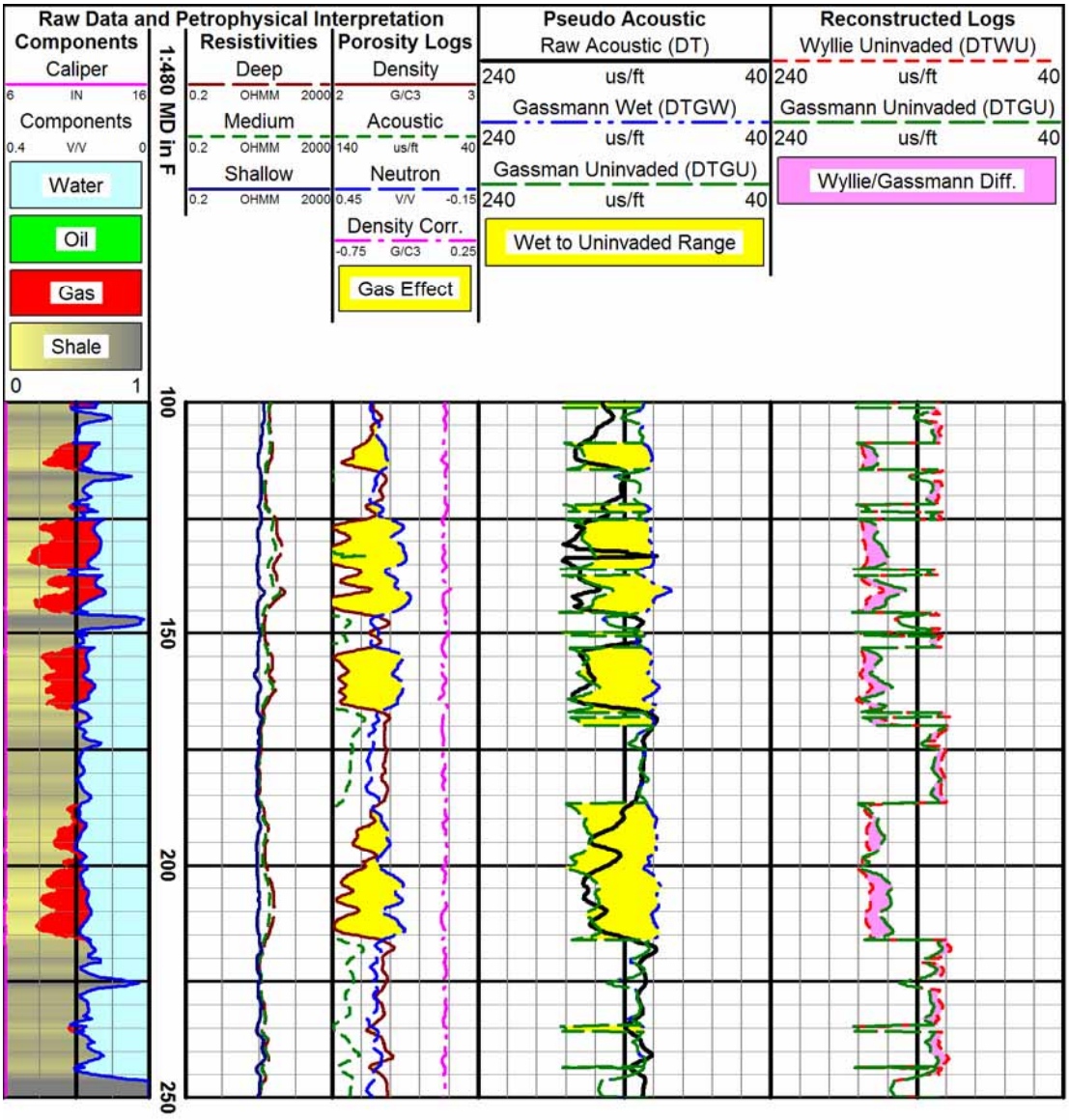

Figure 14 - CSM Strat Test #61. The difference between DT_{GU} and DT_{GW} is approximately 50 microseconds per foot. The actual DT is close to DT_{GU} in all gas (actually air) bearing sands.

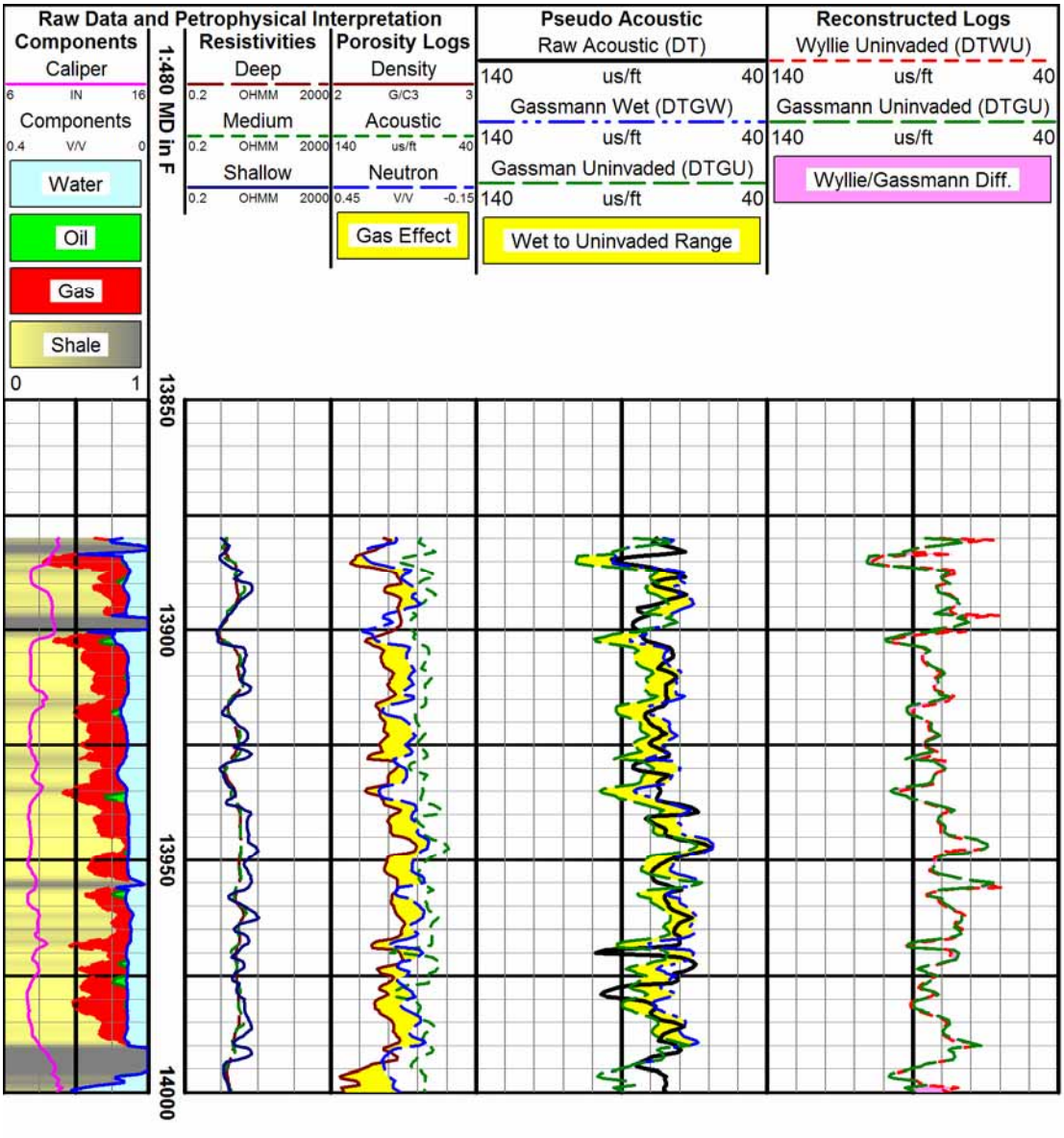

Figure 15 - Cameron Parish Louisiana. The difference between DT_{GU} and DT_{GW} is approximately 10 microseconds per foot. The actual DT meanders between DT_{GU} and DT_{GW}.

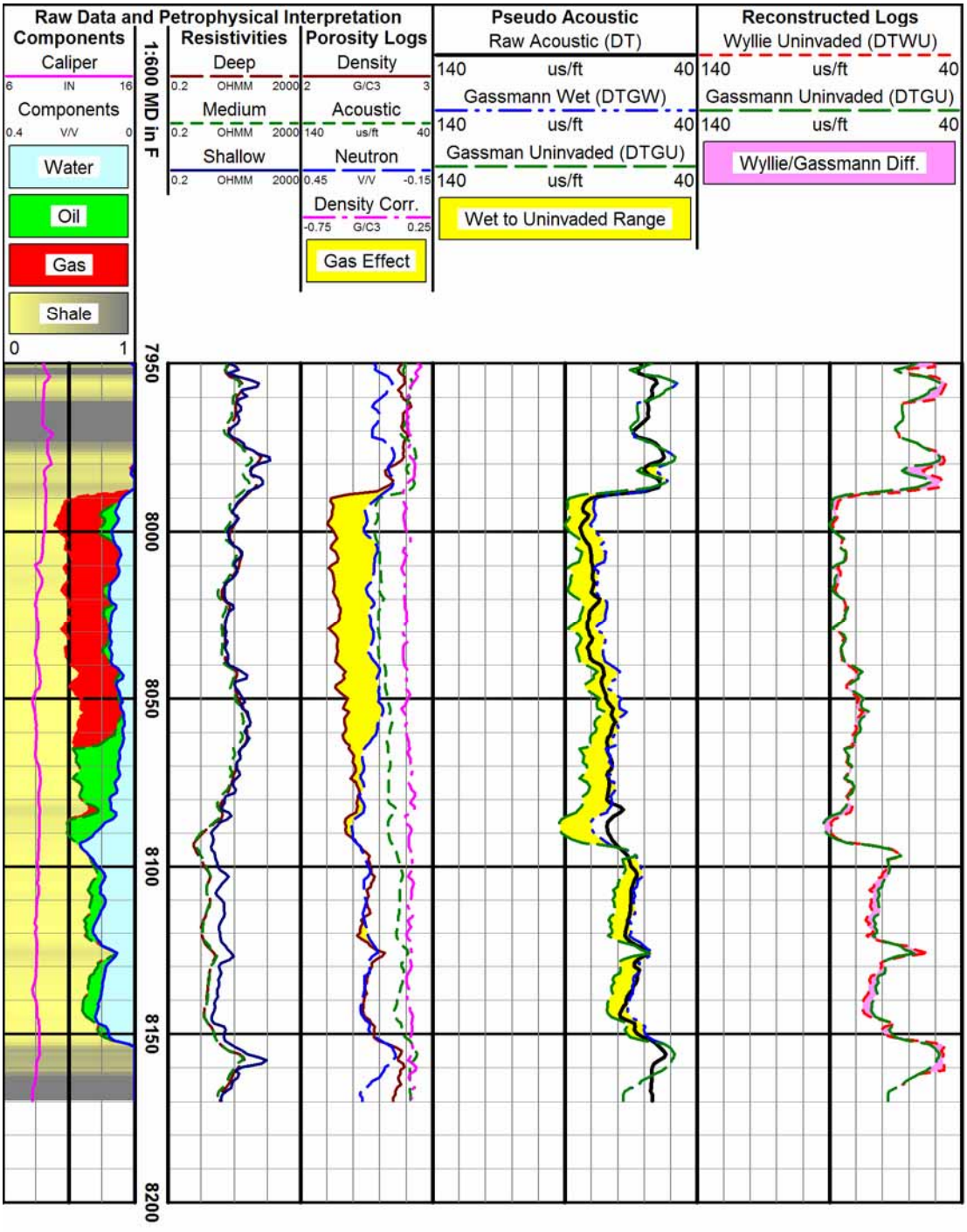

Figure 16 - LA-Lime. The difference between DT_{GU} and DT_{GW} is approximately 10 microseconds per foot. The actual DT meanders between DT_{GU} and DT_{GW} in the gas zone, and is the same as DT_{GW} in the water zones.

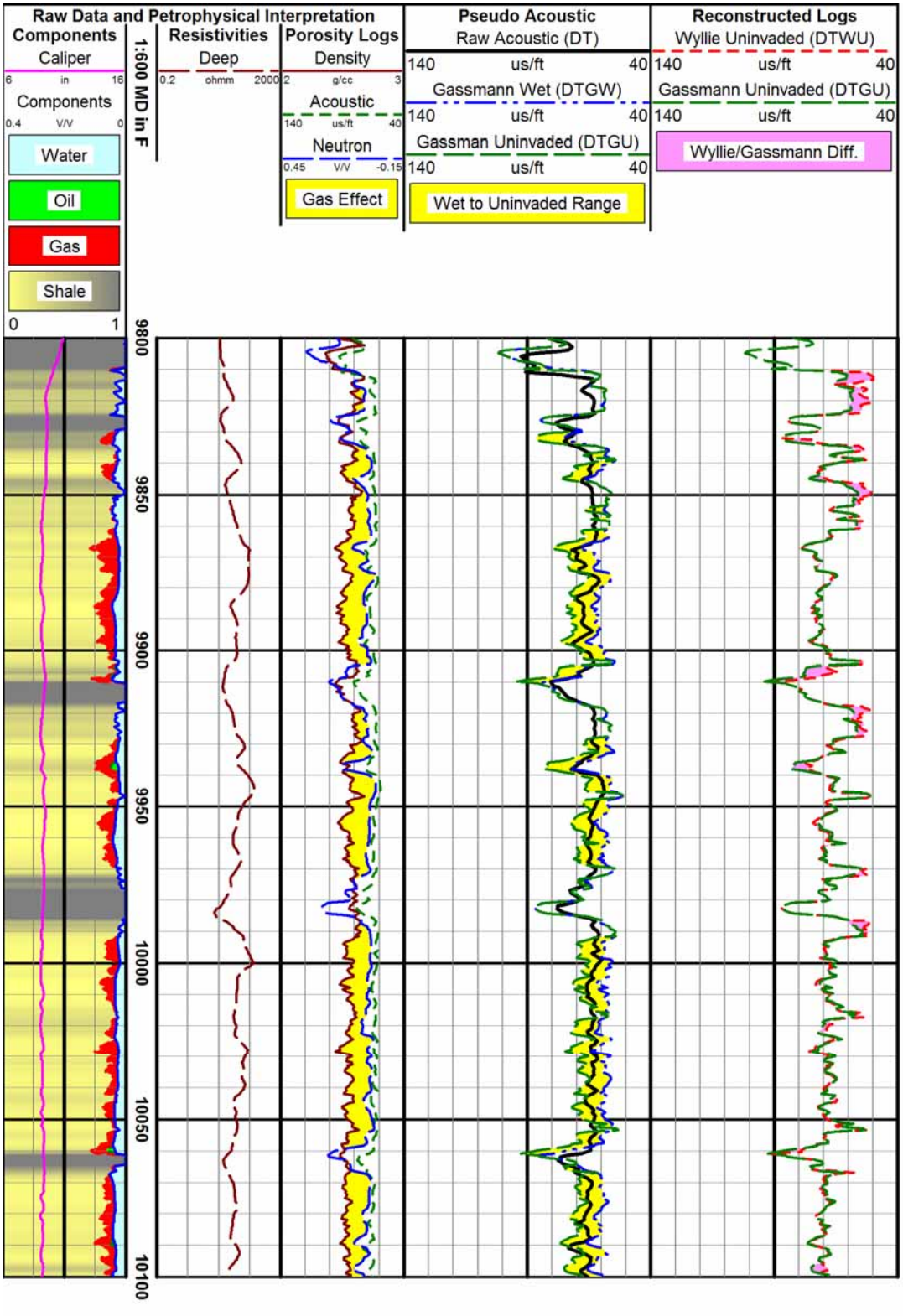

Figure 17 - Wamsutter. The difference between DT_{GU} and DT_{GW} is approximately 10 microseconds per foot. The actual DT meanders between DT_{GU} and DT_{GW}.